Molecular encapsulation of 5-nitroindazole derivatives in 2,6-dimethyl-β-cyclodextrin: Electrochemical and spectroscopic studies

Fernanda Pérez-Cruz [a], Carolina Jullian [a,*], Jorge Rodriguez [b,c], Vicente J. Arán [d], Claudio Olea-Azar [b,*]

[a] Departamento de Química Orgánica y Fisicoquímica, Facultad de Ciencias Químicas y Farmacéuticas, Universidad de Chile, Casilla 233, Santiago 1, Chile
[b] Departamento de Química Inorgánica y Analítica, Facultad de Ciencias Químicas y Farmacéuticas, Universidad de Chile, Casilla 233, Santiago 1, Chile
[c] Departamento de Química, Facultad de Ciencias Básicas, Universidad Metropolitana de Ciencias de la Educación, Santiago, Chile
[d] Instituto de Química Médica, CSISC, Juan de la Cierva 3, 28006 Madrid, Spain

ARTICLE INFO

Keywords:
5-Nitroindazole
Cyclodextrin
Molecular modeling
NMR
ESR

ABSTRACT

Four different 5-nitroindazole derivatives (**1**–**4**) and its inclusion with Heptakis(2,6-di-*O*-methyl)-β-cyclodextrin (DMβCD) were investigated. The stoichiometric ratios and stability constants describing the extent of formation of the complexes were determined by phase-solubility measurements obtaining in all cases a type-A_L diagram. Also electrochemical studies were carried out, where the observed change in the E_{PC} value indicated a lower feasibility of the nitro group reduction. The same behavior was observed in the ESR studies. The detailed spatial configuration is proposed based on 2D NMR methods. These results are further interpreted using molecular modeling studies. The latter results are in good agreement with the experimental data.

1. Introduction

The American trypanozomiasis is a disease that according to data from WHO, over 24 million people are infected or at least serologically positive for *Trypanosoma cruzi*.[1] The importance of the investigations of nitroheterocycles derivatives lie in the existence of the group electroacceptor capable of generate radicals species (ROS) that act against the parasite producing oxidative stress. Since 2005 there began the study of a family of 5-nitroindazole (NI) derivatives in order to verify their anti-trypanocidal activity. A recent study has shown the in vitro and in vivo anti-trypanosomatide activity,[2] besides, the mode of action of the NI against *T. cruzi* has being reported by the first time.[3] Recently, the electrochemical study and the generation of the nitro anion radical of 5-nitroindazole derivative was done.[4] Unfortunately many of these compounds showed low water solubility, which is a problem for its possible use as antichagasic drugs.

Cyclodextrins (cyclic oligosaccharides composed of D-glucose units) (Scheme 1) are known for their ability to bind non-covalently and forming inclusion complexes with wide variety organic compounds.[5] In these complexes, a guest molecule is held within the lipophilic cavity of a cyclodextrin host molecule. The cyclodextrin cavity has an apolar character similar to an 80% dioxane/water solution and provides a slightly alkaline environment, because it is surrounded by glycosidic ethers.[6] The main driving force of the complexation is the release of enthalpy-rich water molecules from the cavity.[7–11] Replacement of water molecules by more hydrophobic guest molecules present in the solution results in formation of an inclusion complex between the host and the guest.[12]

In a previous work[13] we verified that the incorporation of NI derivatives in cyclodextrins improved their solubility. In this sense, encapsulating the drug in the hydrophobic cavity of cyclodextrin seems to be a good approximation in order to increase the bioavailability and biological activity.

In this work, inclusion complex of four 5-nitroindazole derivatives in Heptakis(2,6-di-*O*-methyl)-β-cyclodextrin molecule were prepared in order to improve the aqueous solubility of the drugs. The inclusion complexes were analyzed by UV–vis, NMR spectroscopy, Differential pulse polarography, ESR and molecular modeling techniques. The structural information obtained and the geometry of the complexes, are necessary to clarify the complexation mechanism and the importance of the substituent groups on the indazole ring.

2. Results and discussion

The stoichiometric ratios and stability constants were derived from the changes in the solubility of the substrates **1–4** (Scheme 1) in the presence of increasing amounts of DMβCD, measured by

* Corresponding authors.
E-mail address: cjullian@uchile.cl (C. Jullian).

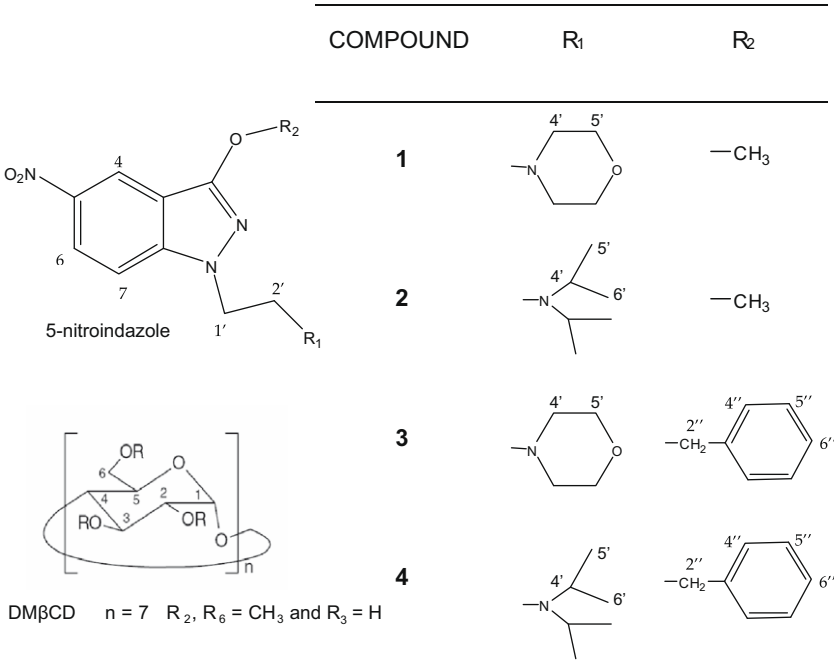

Scheme 1.

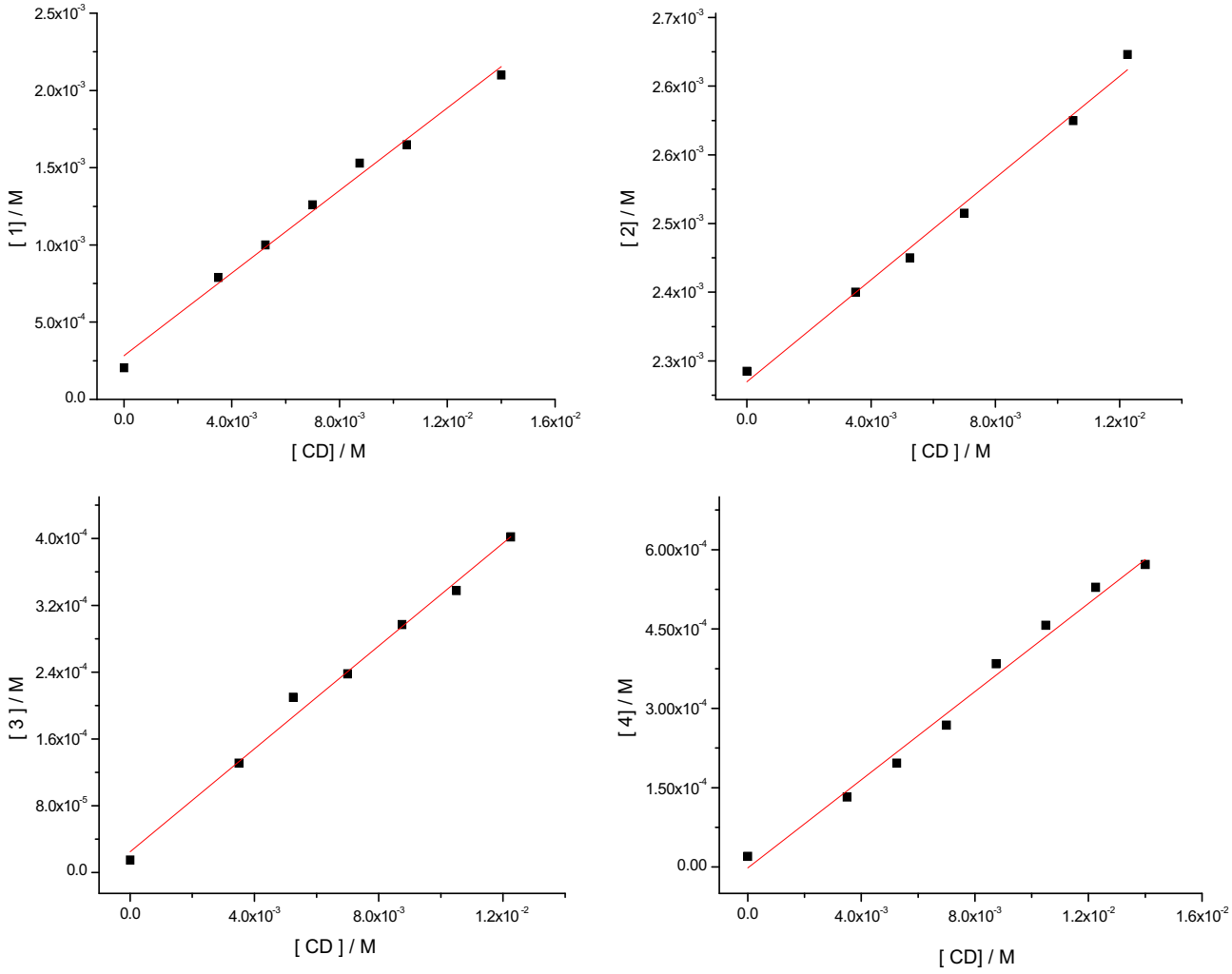

Figure 1. Phase solubility diagrams of compounds **1**–**4** with DMβCD in water at 30 °C.

Table 1
Association constants for NI–DMβCD complexes

Inclusion complex	K_a (M^{-1})	r
1:DMβCD	542 ± 8	0.985
2:DMβCD	14 ± 11	0.985
3:DMβCD	8955 ± 15	0.989
4:DMβCD	2145 ± 12	0.995

UV–vis spectroscopy. For all the NI/DMβCD systems, cyclodextrin enhance the aqueous solubility of NI derivatives, as shown in Figure 1. The binding constant K_a of the complexes was calculated from the slopes of the linear phase-solubility plots, Table 1, according to the methodology described in the experimental part. These diagrams showed a linear relationship between the amount of NI solubilized and the concentration of CD in solution.

The binding constant for the nitroindazole derivatives with DMβCD followed the rank order **3** > **4** > **1** > **2**, reflecting an enhancement of binding on the different substituent's of the nitroindazole derivative. We observed previously the same trend employing βCD instead of DMβCD[14] (data not shown), but with less association constants, indicating that the complexation ability of the β-cyclodextrin is significantly enhanced by its methylation. Apparently, the presence of the methylated groups in the cyclodextrin, seems to be important for the binding of these compounds in the cyclodextrin cavity.[13,15] These groups enlarge the cyclodextrin cavity, making its environment more hydrophobic and favor the adaptability of the cyclodextrin towards a guest, through an enhanced flexibility.

Also, the enhancement of the K_a values can be related to the different substituent groups at the positions R1 and R2 of the indazole ring. In this regards, morpholine and benzyloxy groups have a positive influence on the association constant and isopropyl and methoxyl groups have a negative influence on the K_a value.

On the other hand, the ratio R was plotted against the difference of the absorbance of NI in presence and absence of DMβCD. The results of Job's plot are shown in Figure 2. According to the continuous variation method, the maximum concentration of the complex will be present in the sample where the molar ratio R corresponds to the complexation stoichiometry. The maximum absorbance variation for DMβCD with the nitroindazole **1**–**4** derivatives was observed for R = 0.5, which might indicate that the main stoichiometry is 1:1, in agreement with the stoichiometry suggested from the phase-solubility study.

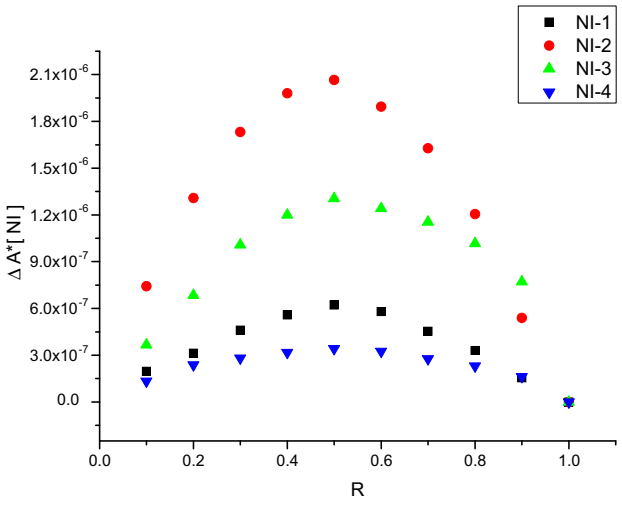

Figure 2. Continuous variation plot for the complexes **1**, **2**, **3**, **4** with DMβCD from absorbance measurements.

2.1. Differential pulse polarography (DPP) studies

Electrochemical behavior in protic media for this kind of 5-nitroindazole derivatives has been previously studied,[3,13] indicating that NI derivatives are able to be reduced on the mercury electrode due to the four-electron and four-proton irreversible reduction of the nitroaromatic moiety to yield the hydroxylamine derivative according to the following overall reaction:

$$R{-}NO_2 + 4e^- + 4H^+ \rightarrow R{-}NHOH + H_2O \quad (1)$$

Consequently to evaluate changes in the polarograms, due to addition of DMβCD into a solution of NI, we used different NI/DMβCD mixtures in aqueous media at pH 7.4. The addition of DMβCD to a solution of NI causes two main changes in the polarograms. Firstly, the cathodic peak potential (E_{PC}) shifted in a negative direction and secondly, the cathodic peak current I_{PC} increased. Figures 3 and 4, show the displacement of cathodic peak potential (E_{PC}) for compounds **3** and **4**, when different concentrations of DMβCD are used. The shift of signals **4**-DMβCD and **3**-DMβCD to more negative potentials indicates that the nitro group is reduced less favorably when the indazole ring is included in the hydrophobic cavity hindering the interaction with the electrode. Complexes **3**-DMβCD and **4**-DMβCD show very close reduction potentials, −0.57 V and

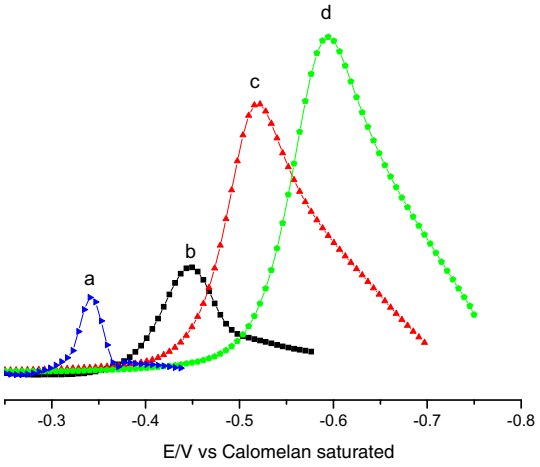

Figure 3. DPP of 1 mM **4** in 0.1 M of phosphate buffer pH 7.4. Compound **4** in (a) absence and presence of (b) 2, (c) 6 and (d) 8 mM DMβCD. Conditions: scan rate 10 mV s^{-1}, pulse amplitude 50 mV, pulse width 50 ms.

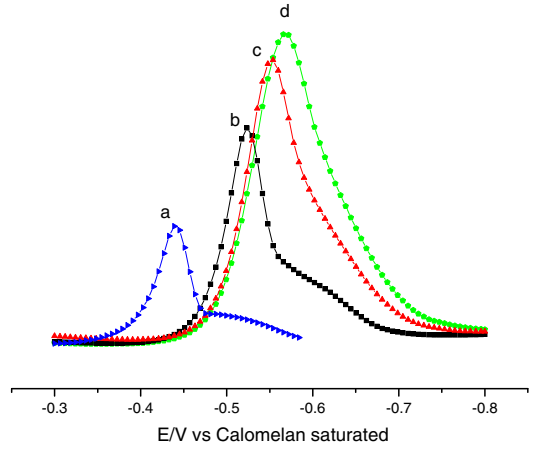

Figure 4. DPP of 1 mM **3** in 0.1 M of phosphate buffer pH 7.4. Compound **3** in (a) absence and presence of (b) 2, 6 (c) and (d) 8 mM DMβCD. Conditions: scan rate 10 mV s^{-1}, pulse amplitude 50 mV, pulse width 50 ms.

Table 2
Reduction potential of NI derivatives with and without DMβCD in DMSO versus SCE

Compound	E_{PC} without CD	E_{PC} with 8 mM CD	ΔE
1	−0.54	−0.60	−0.06
2	−0.59	−0.62	−0.03
3	−0.44	−0.57	−0.13
4	−0.34	−0.59	−0.25

−0.59 V, respectively (Table 2). This result indicated that the inclusion mode for both compounds will be similar and the different values of K_a will be also related with the different substituent. On the other hand, the NI–DMβCD reduction potentials around to −0.60 V suggest that the NI complexation would not decrease the biological activity of NI. Previous report has indicated that nitrocompounds are reduced with reduction potentials values between −0.33 V and −0.65 V (vs SCE, in phosphate buffer pH 7).[16]

The other effect, the increment of the cathodic peak current could be explained by the autoprotonation mechanism observed previously.[17] The highly apolar medium of the cyclodextrin cavity displace the equilibrium of the reaction 1 to the formation of the hydroxylamine products. This is confirmed with the result for compound **2**, where no signal increased was detected (Fig. 5.)

2.2. Electro spin resonance (ESR) studies

In order to stabilize the nitro anion radical form of these compound we worked using an aprotic medium (DMSO and PTBA as supporting electrolyte) in the electrochemical reductions (electrolysis to controlled potential in situ) to generate radical form. All the studied structures produced stable paramagnetic intermediates at the first reduction step. The interpretation of the ESR spectra by means of a simulation process led to the determination of the experimental coupling constants for the observed magnetic nuclei. The ESR spectra of the four nitroindazole derivative **1**, **2**, **3** and **4** have the same hyperfine pattern. The ESR spectra, Figure 6, were analyzed and simulated in term of one triplet that is assigned to the nitrogen atom of the nitro group (a_{NO2} = 11.35 G), three doublets due to hydrogen's 4, 6 and 7 of the indazole moiety (a_{H4} = 5.5 G, a_{H6} = 2.0 G, a_{H7} = 1.1 G) and two triplet due to the Nitrogen's of indazole ring (a_N = 0.2 G, a_N = 0.45 G). The electrochemistry reduction of nitroindazole derivatives were generated in presence of DMβCD, however, not ESR signal were register (data not shown).

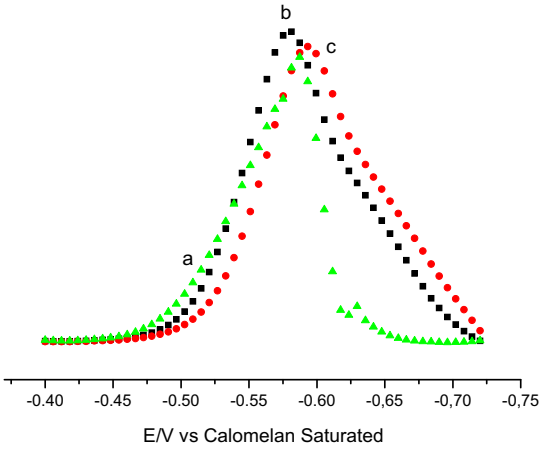

Figure 5. DPP of 1 mM **2** in 0.1 M of phosphate buffer pH 7.4. Compound **2** in (a) absence and presence of (b) 2, and (c) 6 mM DMβCD Conditions: scan rate 10 mV s^{-1}, pulse amplitude 50 mV, pulse width 50 ms.

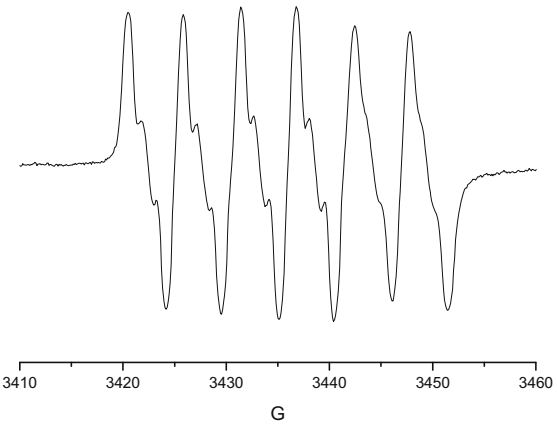

Figure 6. ESR experimental spectrum of the radical-anion of compound **3** in DMSO.

2.3. Nuclear magnetic resonance (NMR) studies

NMR studies allowed us to distinguish between inclusion and other possible external interaction processes. In fact, NMR is the most powerful technique used to determine the inclusion of a guest molecule into the hydrophobic CD cavity, in solution. It is well known that the chemical shifts of the hydrogen atoms located in the interior of the CD cavity (H-3 and H-5) become shielded and usually show significant upfield shift in the presence of a guest molecule, whereas the hydrogen atoms on the outer surface (H-1, H-2 and H-4) are not affected or experience only a marginal shift upon complexation.

Reasonably water solubility (>0.014 mM) for compounds **1**–**4** of the complex at 30 °C gave feasible ^{1}H NMR spectra performed in D_2O, thus providing further experimental evidence of the complex formation because free NI derivatives are practically water insoluble. Table 3 lists the detailed variation of the chemical shifts of compounds **1, 2, 3** and **4** and internal protons of cyclodextrin before and after forming inclusion complex. The induced shift $\Delta\delta$ is defined as the difference in chemical shift in the absence and presence of the other reactants. In the present case, the induced shifts were calculated by the following equation: $\Delta\delta = \delta_{(free)} - \delta_{(complex)}$. In this convention, positive and negative signs show high and low frequency shifts, respectively. In order to determine the chemical shift of the protons that are superimposed in the CD region, an HSQC (heteronuclear single quantum correlation) spectrum of the complex was performed.

Table 3
Difference in chemical shift of NI–DMβCD complexes in D_2O

	$\Delta\delta = \delta_{free} - \delta_{bound}$			
H	**1**	**2**	**3**	**4**
4	0.17	0.09	0.08	0.13
6	0.13	0.07	0.03	0.01
7	0.02	−0.03	−0.05	0.03
1′	0.06	0.03	0.04	0.03
2′	nd	0.05	0.13	0.00
4′	−0.03	0.03	−0.41	0.04
5′	−0.02	0.00	0.87	0.03
6′	–	0.00	–	0.03
2″	−0.03	−0.03	0.00	−0.01
4″	–	–	0.05	0.09
5″	–	–	0.05	−0.04
6″	–	–	0.02	0.04
DMβCD				
H-3	0.12	0.28	0.05	0.17
H-5	0.07	0.09	0.04	0.14
H-6	0.00	0.00	0.01	0.03

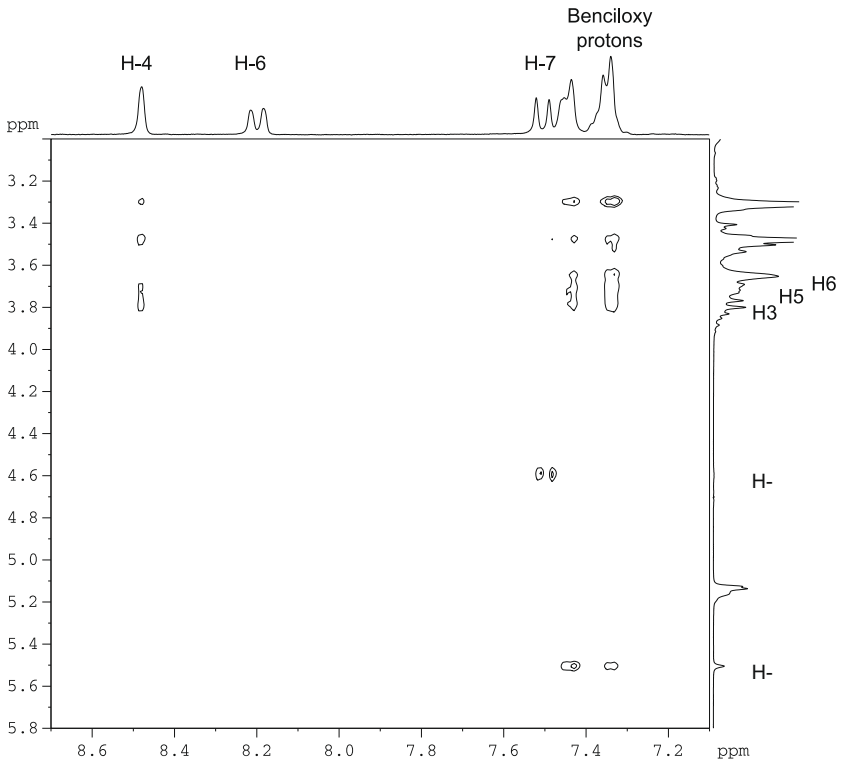

Figure 7. Partial contour plot of two-dimensional ROESY spectrum of **3**-DMβCD inclusion complex.

All the **1, 2, 3** and **4** protons showed frequency changes in the presence of DMβCD (Table 3). The signals of H-4 and H-6 displayed upfield frequency changes in more extent for **1**, than the other nitroindazole derivative. The movements of these proton signals suggested that the penetration of the substrate involves insertion of the nitroindazole ring portion inside the cavity. This interpretation is supported by the strong displacement of the H-3 and H-5 protons of the annular interior of DMβCD. This displacement is due to the anisotropic magnetic effect induced by the presence of the aromatic group of the guest molecule. Since the signal due to H-6, which is located at the narrow end of the cyclodextrin, is not significantly shielded by the guest molecule, it is likely that the NI molecules enters from the wider end of the cyclodextrin where the secondary hydroxyls are located.

Further information about the inclusion mode of NI derivative in the cyclodextrin cavity can be derived from the evidence of spatial proximities between protons of CD and NI. Two-dimensional (2D) NMR is a powerful tool for investigating inter- and intra-molecular interaction. The presence of NOE cross-peaks between protons from two species indicates spatial contacts within 0.4 nm. To gain more conformational information, we used 2D-ROESY to study the inclusion complexes and the effects were only qualitatively used. These studies were carried out only for compounds **3** and **4** due to the low solubility of the complexes **1**-DMβCD and **2**-DMβCD.

The presence of cross-peak between nitroindazole and cyclodextrin hydrogen as detected in the 2D-ROESY experiments, could only arise if a **3**-DMβCD complex has been formed. The cross-peaks between H-4 of **3** with H-3, H-5 hydrogen of DMβCD in Figure 7 suggests a geometry of complexation where the aromatic part of the nitroindazole ring is inserted in the cyclodextrin cavity by the wide side. The aliphatic chain with morpholine (R1) is folded over the aromatic moiety due to the intramolecular interaction observed between H7 and H-1′ which is in accordance with the geometry obtained by the ROESY spectrum of **3** in solution (data not shown) and with the large shift changes observed for the morpholine protons due to the anisotropic effect of the nitroindazole ring (Table 3). On the other hand, the cross-peaks observed between the benzyloxy protons and H-6/H-5 of the cyclodextrin indicate that this group is near the primary rim.

Figure 8 depicts the ROESY spectrum for **4**-DMβCD, where the interaction between H-4 of the nitroindazole ring and the hydrogens of the benzyl group with the hydrogen H-5/H-6 of the DMβCD revealed that the nitroindazole moiety is in the DMβCD. Whereas the aliphatic chain, R1, is also inserted in the cyclodextrin cavity due to the interaction observed between the isopropyl hydrogen with H-5 of the cyclodextrin (data not shown), this means that the insertion of compound **4** in the cyclodextrin cavity is deeper than compound **3**, which is in accordance to our DPP results.

In order to rationalize our experimental results described above, we carried out molecular modeling studies of the complexes. These studies revealed a preferred final orientation for all the complexes studied, in spite of the different initial configuration arbitrarily imposed.

The conformation obtained by molecular modeling was in agreement with the ROESY results. The **3**-DMβCD complex has the nitroindazol derivative inserted in the cyclodextrin cavity with the morpholine group folded over the indazole ring closer the secondary rim, while the benzyloxy ring remain oriented to the primary rim. For instance, H-4 of the compound **3** is nearby to H-3 and H-5 of DMβCD which display distances lower than 2.0 Å, Figure 9, this is in agreement with the observed cross-peak of the 2D-ROESY spectrum of **3**-DMβCD, Figure 7.

For the other complexes **1**, **2** and **4** the same form of inclusion is observed. Concerning R2 group is oriented to the primary rim and R1 is oriented to the secondary rim. This is in agreement with our previous work[13] where for the same cyclodextrin the methyl group (R2) is oriented to the narrow end and the dimethyl amine (R1) is orientated toward secondary rim.

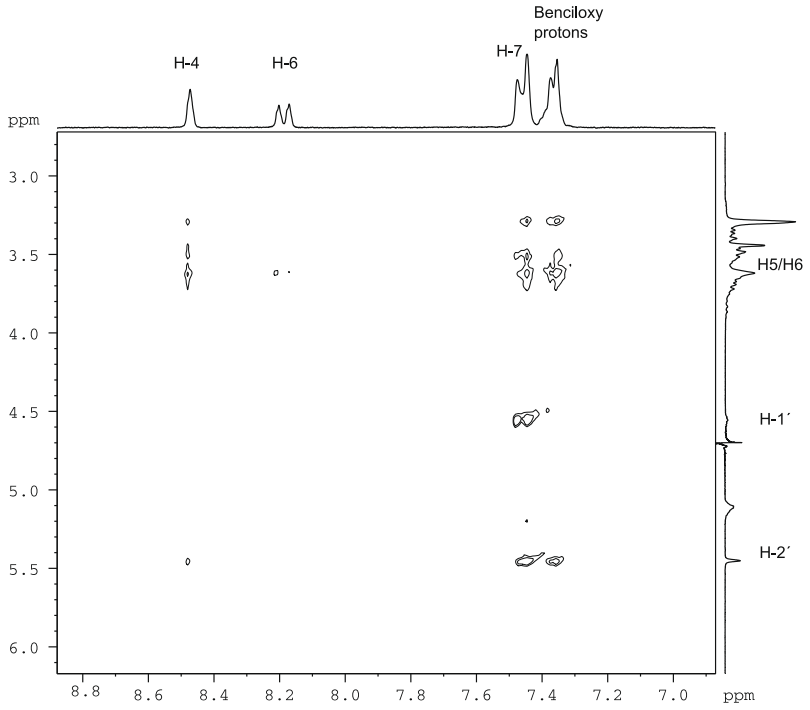

Figure 8. Partial contour plot of two-dimensional ROESY spectrum of **4**-DMβCD inclusion complex.

3. Conclusion

The aqueous solubility of the four nitroindazole derivatives studied has been improved in neutral aqueous solution through complexation with DMβCD. These results indicated interaction between NI and DMβCD in water forming 1:1 inclusion complex. The binding constant followed the rank order **3** > **4** > **1** > **2**, reflecting an enhancement of binding on the different substituent's of the nitroindazole derivative.

The effect of DMβCD on the polarographic behavior of nitroindazole derivative can be summarized in a negative shift in the cathodic peak potential for compounds **1**, **3** and **4** and with a less extend compound **2**, and an enhancement of the cathodic peak current probably due to an autoprotonation mechanism product of the inclusion of the nitroindazole in the cyclodextrin cavity.

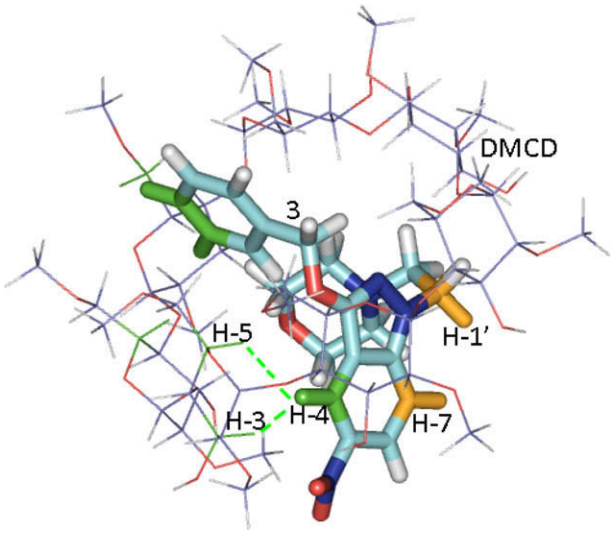

Figure 9. Molecular modeling for the complex **3**-DMβCD.

The NMR and molecular modeling studies reveal that the inclusion of nitroindazole is by the wide side of the cyclodextrin cavity and the R2 group is oriented to the primary rim and R1 is oriented to the secondary rim.

4. Experimental

4.1. Reagents

The 5-NI derivatives **1–4**, Scheme 1 were synthesized according to methods described earlier.[18] Compound **1**: 3-methoxy-1-(2-morpholineethyl)-1*H*-indazole, compound **2**: *N*-isopropyl-*N*-(2-(3-methoxy-1*H*-indazol-1-yl)ethyl)propan-2-amine, compound **3**: 3-(benzyloxy)-1-(2-morpholinoethyl)-1*H*-indazole, compound **4**: *N*-(2-(3-(benzyloxy)-1*H*-indazol-1-yl)ethyl)-*N*-isopropylpropan-2-amine.

The reagents β-cyclodextrin (βCD), heptakis(2,6-di-*O*-methyl)-β-cyclodextrin (DMβCD), and deuterated water (D_2O) were purchased from Sigma–Aldrich, Inc., St. Louis, MO. Other reagents were all analytical grade and double distilled water was used throughout.

4.2. Phase-solubility measurements

Phase-solubility measurements were carried out according to the method of Higuchi and Connors[19] excess amount of NI (5 mg) was added to 5 mL of deionized water containing increasing amounts of DMβCD (ranging from 0 to 0.014 M). The resulting mixture was equilibrated in a Julabo thermostatic shaking water bath for 24 h at 30 °C after which the equilibrium was reached. The suspensions were filtered through 0.45 μm cellulose acetate membrane filter to remove undissolved solid. An aliquot from each vial was adequately diluted and spectrophotometrically analyzed at 362 nm. The presence of DMβCD did not interfere in the spectrophotometric assay of NI–DMβCD.

The apparent stability constant (K_a) of the complexes was calculated from the phase-solubility diagrams according to the following equation:

$$K_a = \frac{\text{slope}}{S_o(1 - \text{slope})} \quad (2)$$

where S_o is the solubility of NI at 30 °C in the absence of cyclodextrin and slope means the corresponding slope of the phase-solubility diagrams, that is, the slope of the drug molar concentration versus CDs molar concentration graph.

4.3. Stoichiometry determination by the continuous variation method (Job's plot)

The stoichiometry of inclusion was determined by the method developed by Job.[20] Equimolar solutions of NI and CD were mixed to a standard volume varying the molar ratio but keeping the total concentration of the species constant. After stirring for 24 h, the absorbance at 362 nm was measured for all solutions and $\Delta A = A - A_o$, the difference in absorbance in the presence and in the absence of CDs, was plotted against R; R = [NI]/([NI] + [CD]).

4.4. DPP

This technique was used to study the variation of reduction potential of NI for effect of inclusion of NI in cyclodextrins. In protic media, the solutions were prepared starting from a stock solution 0.1 M of sample, NI, in DMSO. The final solution was prepared through the corresponding dilution to obtain a sample final concentration, on the voltammetric cell, of 1.0 mM. DPP experiments were carried out using a Metrohm 693VA instrument with a 694VA Stand convertor and a 693VA Processor, keeping the concentration 1.0 mM of NI in phosphate buffer (0.1 M pH 7.4) constant while varying the concentrations of CDs (0–10 mM), under a nitrogen atmosphere at room temperature, using a three electrode cell. A hanging mercury drop electrode was used as the working electrode, a platinum wire as the auxiliary electrode, and saturated calomel as the reference electrode, 0.1 M KCl used as supporting electrolyte for PPD experiments.

4.5. NMR spectroscopy

One-dimensional ^{1}H NMR spectra were recorded at 300 K on a Bruker Avance DRX operating at a proton NMR frequency of 300.13 MHz in unbuffered D_2O solutions. Acquisition parameters consisted of a spectral width of 3000 Hz, an acquisition time of 2.67 s and a relaxation delay of 1 s. 128 scans were recorded. FIDs were Fourier transformed with LB = 0.3 Hz and GB = 0. The resonance at 4.7 ppm due to residual solvent (HOD) was used as internal reference.

Rotating-frame Overhauser Effect SpectroscopY (ROESY) spectra were acquired in the phase sensitive mode using the same spectrometer and Bruker standard parameters (pulse program roesygpph19). Each spectrum consisted of a matrix of 16 K (F2) by 8 K (F1) points covering a spectral width of 3000 Hz. Spectra were obtained from the samples solutions prepared for the ^{1}H NMR studies, using a spin-lock mixing time of 400 ms, relaxation delay 2 s, and 32 scans were recorded.

4.6. ESR spectroscopy

ESR spectra were recorded in the X band (9.7 GHz) using a Bruker ECS 106 spectrometer with a rectangular cavity and 50 kHz field modulation. The hyperfine splitting constants were estimated to be accurate within 0.05 G. The anion radicals were generated by electrolysis to controlled potential in situ using DMSO as solvent and PTBA as supporting electrolyte. All experiments were carried out at room temperature and under nitrogen atmosphere. The concentration of NI used corresponds to 0.001 M. The ESR spectra were simulated using the program WINEPR Simphonia 1.25 version.

4.7. Molecular modeling

In silico build-up of DMβCD was carried out using the Builder module of the INSIGHTII program[21] by adding to βCD 14 methyl in positions 2 and 6. The obtained model was subjected to optimization using a protocol of 300 steps of conjugate gradients to avoid steric hindrance and clashes that can appear in the building process. The 5-NI derivatives were built using GaussView 3.0 and then they were optimized using a semiempirical method such as AM1 as implemented in GAUSSIAN′ 03 package of programs.[22] ESP charge were obtained employing a single point with B3LYP/6-31G* as methodology of calculation, implemented in the SPARTAN 02′ program.[23,24] The AUTODOCK 04′[25] parameters used for the global search was an initial population of 150 individuals, with a maximal number of energy evaluations of 15,000,000 and a maximal number of generations of 100,000 as an end criterion. An elitism value of 1 was used, and a probability of mutation and crossing-over of 0.02 and 0.08 was used, respectively.

Acknowledgments

The authors are grateful to CSIC 16/07-08, Fondecyt 1071068 and 11080038, UMC-0204 and to CEPEDEQ from Chemical and Pharmaceutical Science Faculty of University of Chile for the use of NMR and ESR equipment.

References and notes

1. World Health Organization (OMS), Report of the Scientific Working Group on Chagas Disease, Buenos Aires, Argentina, 2005.
2. Boiani, L.; Gerpe, A.; Arán, V. J.; Torres de Ortiz, S.; Serna, E.; Vera de Bilbao, N.; Sanabria, L.; Yaluff, G.; Nakayama, H.; Rojas de Arias, A.; Maya, J. D.; Morello, J. A.; Cerecetto, H.; González, M. *Eur. J. Med. Chem.* **2008**. doi:10.1016/j.ejmech.2008.06.024.
3. Rodríguez, J.; Gerpe, A.; Aguirre, G.; Kemmerling, U.; Piro, O. E.; Arán, V. J.; Maya, J. D.; Olea-Azar, C.; González, M.; Cerecetto, H. *Eur. J. Med. Chem.* **2008**. doi:10.1016/j.ejmech.2008.07.018.
4. Rodríguez, J.; Olea-Azar, C.; Barriga, G.; Folch, C.; Gerpe, A.; Cerecetto, H.; González, M. *Spectrochim. Acta Part A* **2008**, *70*, 557.
5. Del Valle, M. E. M. *Proc. Biochem.* **2004**, *39*, 1033.
6. Bender, M. L., Komiyama, M., Eds.Cyclodextrin Chemistry; Springer: Berlin, 1978.
7. Agostiano, A.; Catucci, L.; Cosma, P.; Fini, P. *Phys. Chem. Chem. Phys.* **2003**, *5*, 2122.
8. Baglole, K. N.; Boland, P. G.; Wagner, B. D. *J. Photochem. Photobiol. A* **2005**, *173*, 230.
9. Cosma, P.; Catucci, L.; Fini, P.; Dentuto, P. L.; Agostiano, A.; Angelini, N. *J. Photochem. Photobiol.* **2006**, *82*, 563.
10. Fini, P.; Loseto, R.; Catucci, L.; Cosma, P.; Agostiano, A. *Bioelectrochemistry* **2007**, *70*, 44.
11. Wagner, B. D.; MacDonald, P. J. *J. Photochem. Photobiol. A* **1998**, *114*, 151.
12. Verrone, R.; Catucci, L.; Cosma, P.; Fini, P.; Agostiano, A.; Lippolis, V. *J. Inclusion Phenom. Macrocycl. Chem.* **2007**, *57*, 475.
13. Jullian, C.; Morales-Montecinos, J.; Zapata-Torres, G.; Aguilera, B.; Rodriguez, J.; Arán, V.; Olea-Azar, C. *Bioorg. Med. Chem.* **2008**, *16*, 5078.
14. Ungraduated Thesis, Fernanda Pérez C. 'Electrochemical Study of 5-Nitroindazole Derivatives and Spectroscopic Analysis of their Inclusion Complexes with Cyclodextrin' Chemical and Pharmaceutical Science Faculty of University of Chile.
15. de Melo, N. F. S.; Grillo, R.; Rosa, A. H.; Fraceto, L. F. *J. Pharm. Biomed. Anal.* **2008**, *47*, 865.
16. Livertoux, M. H.; Lagrange, P.; Minn, A. *Brain Res.* **1996**, *725*, 207.
17. Olea-Azar, C.; Cerecetto, H.; Gerpe, A.; Gonzalez, M.; Arán, V. J.; Rigol, C.; Opazo, L. *Spectrochim. Acta Part A* **2006**, *63*, 36.
18. Rodríguez, J; Arán, V. J.; Aguirre, G.; Olea-Azar, C.; González, M.; Cerecetto, H.; Maya, J. D.; Carrasco, C.; Speisky, H., in preparation.
19. Higuchi, T.; Connors, K. A. *Adv. Anal. Chem. Inst.* **1965**, *4*, 117.
20. Job, P. *Ann. Chim.* **1928**, *9*, 113.
21. InsightII, MSI, San Diego, California.
22. Frisch, M. J.; Trucks, G. W.; Schlegel, H. B.; Scuseria, G. E.; Robb, M. A.; Cheeseman, J. R.; Zakrzewski, V. G.; Montgomery, J. A.; Stratmann, R. E.; Burant, J. C.; Dapprich, S.; Millam, J. M.; Daniels, A. D.; Kudin, K. N.; Strain, M. C.; Farkas, O.; Tomasi, J.; Barone, V.; Cossi, M.; Cammi, R.; Mennucci, B.; Pomelli, C.; Adamo, C.; Clifford, S.; Ochterski, J.; Petersson, G. A.; Ayala, P. Y.; Cui, Q.; Morokuma, K.; Rega, N.; Salvador, P.; Dannenberg, J. J.; Malick, D. K.; Rabuck, A. D.; Raghavachari, K.; Foresman, J. B.; Cioslowski, J.; Ortiz, J. V.; Baboul, A. G.;

Stefanov, B. B.; Liu, G.; Liashenko, A.; Piskorz, P.; Komaromi, I.; Gomperts, R.; Martin, R. L.; Fox, D. J.; Keith, T.; Al-Laham, M. A.; Peng, C. Y.; Nanayakkara, A.; Challacombe, M.; Gill, P. M. W.; Johnson, B.; Chen, W.; Wong, M. W.; Andres, J. L.; Gonzalez, C.; Head-Gordon, M.; Replogle, E. S.; Pople, J. A., Gaussian, Inc., Pittsburgh, PA, 2001.

23. PC Spartan '04 User's Guide; Wavefunction Inc: California.
24. Wavefunction Inc: 18401 Von Karman Avenue, Suite 370, Irvine, California 92612, USA.

[25]. Morris, G. M.; Goodsell, D. S.; Halliday, R. S.; Huey, R.; Hart, W. E.; Belew, R. K.; Olson, A. *J. Comput. Chem.* **1998**, *19*, 1639.